JOURNAL OF INTERNATIONAL CRISIS AND RISK COMMUNICATION RESEARCH
ISSN: 2576-0017
2024, VOL 7, NO S5

Mixed Convection Heat Transfer Inside a Lid-driven Trapezoidal Cavity For $H_2O - Cu - Al_2O_3$ Hybrid Nanofluid

Hamza Ghazi Mohammed[1], Akeel Abdullah Mohammed[2]

1,2.Department of Mechanical Engineering, College of Engineering, Al-Nahrain University, Baghdad, Iraq

Abstract
The mixed convection inside a trapezoidal lid-driven cavity for a circular cylinder heat source was numerically investigated via Ansys commercial program (ANSYS Fluent 2021 R2 and 2022 R1). This study employed two distinct fluids, namely H_2O and $Water - Cu - Al_2O_3$ hybrid nanofluid. The upper wall maintains a steady velocity while the lower wall stays motionless. Both walls remain cold. However, the inclined cavity walls are insulated via adiabatic insulation. The present investigation has undergone validation and comparison with previously published research, yielding a significant degree of correspondence with an average relative difference of around 1.62%. The outcomes comprise of three distinct Richardson number values: 0.01, 1, and 10, radius ratios of 0.20 and 0.25, four inner cylinder positions (center, right, top, bottom), and four inclination angles: 0°, 45°, 90°, and 180°. It is demonstrated that bottom position of (0, −0.12) is the desirable position with the largest mean Nusselt number across the angles (φ = 0°, 45°, and 90°). When the position lies at the top (0, 0.12), and the angle is 180°, the maximum heat transfer rate is achieved.
Keywords: mixed convection, hybrid nanofluid, lid-driven, heat transfer, trapezoidal cavity.

1. Introduction

Mixed convection heat transfer can take place in containers when the top wall, bottom wall, or both walls are in active motion. Authors have shown significant interest in lid-driven containers employing various geometries, boundary conditions, and improvement methods because of their crucial role in industrial applications. Applications of this technology include nuclear reactors, solar energy, and lubrication system technology [1]. The subject of mixed convection within lid-driven cavities was investigated using various heat transfer enhancing methods. Enhancing the base fluid's thermal conductivity by employing nanofluids and hybrid nanofluids [1-18] and porous media [19-29] is a very efficient approach among these methods. Other techniques involves utilizing vibrations or magnetic field within the cavity for various directions, including or excluding the use of nanofluids [30-49].

The current work uses the commercial Ansys program (ANSYS Fluent 2022 R1) to perform a numerical simulation of mixed convection within an inclined trapezoidal cavity that is driven by a lid and filled with an $H_2O - Cu - Al_2O_3$ hybrid nanofluid. The heat source includes a heated circular cylinder that is preserved at a constant temperature of T_h. Both the moving top wall and the fixed bottom wall are subjected to isothermal cooling at a temperature of T_c and the cavity's inclined walls are insulated using adiabatic methods. The upper wall maintains a steady velocity and the remaining walls are fixed. The Richardson number values studied in this work are as follows: (Ri=0.01, 1, and 10). The current work has selected two values for the radius ratio: 0.20 and 0.25, four internal cylinder position (center, bottom, top, right), four values for the inclination angles: 0°, 45°, 90°, and 180° as well as four values for the hybrid nanoparticle volume percentages ϕ = 0%, 4%, 6%, and 8%.

2. Theoretical Model

2.1. Geometrical Configuration and Assumptions

Numerical analysis of trapezoidal cavity heat transfer using two-dimensional, steady, and laminar mixed convection flow is performed. The fluid medium is presumed to be

incompressible and exhibits Newtonian behavior. The Boussinesq approximations are used to describe density-dependent temperature change and connect the temperature and flow fields. The dissipative effect from the viscous component is disregarded here. Heat generation is not accounted for.

Figure 1 graphically illustrates the physical domain of the trapezoid lid-driven system for each case considered in this work. The cavity has two parallel cold walls characterized by a constant temperature T_c. A constant velocity is being maintained within the positive x-direction of the top short wall. Furthermore, the sloped walls are insulated adiabatically. An isothermal heating is applied to the inner cylinder at T_h. This study establishes two radius ratios by considering two different values of the radius of the inner cylinder r_o. The cavity has an inclination angle of φ relative to the x-axis, resulting in an opposed flow condition where the free convection flow induced by the thermally non-homogeneity within the cavity's boundaries is opposed by the shear flow resulting from the moving upper wall.

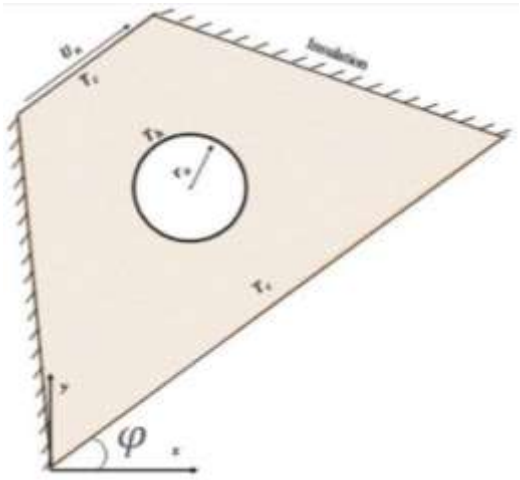

Figure 1. Main Geometry.

2.2. Mathematical Equations and Formulation

In their dimensionless form, the equations of conservation for mass, momentum and energy are [53]:

$$\frac{\partial V}{\partial Y}+\frac{\partial U}{\partial X}=0 \tag{3.1}$$

$$V\frac{\partial U}{\partial Y}+U\frac{\partial U}{\partial X}=-\frac{\partial P}{\partial X}+\frac{1}{Re}\frac{\mu_{hnf}}{\mu_f}\frac{\rho_f}{\rho_{hnf}}\left(\frac{\partial^2 U}{\partial X^2}+\frac{\partial^2 U}{\partial Y^2}\right) \tag{3.2}$$

$$V\frac{\partial V}{\partial Y}+U\frac{\partial V}{\partial X}=-\frac{\partial P}{\partial X}+\frac{1}{Re}\frac{\mu_{hnf}}{\mu_f}\frac{\rho_f}{\rho_{hnf}}\left(\frac{\partial^2 V}{\partial X^2}+\frac{\partial^2 V}{\partial Y^2}\right)+\left(\frac{(\rho\beta)_{hnf}}{\rho_{hnf}\beta_f}\right)Ri\,T^{+} \tag{3.3}$$

$$V\frac{\partial T^{+}}{\partial Y}+U\frac{\partial T^{+}}{\partial X}=\frac{\alpha_{hnf}}{\alpha_f}\frac{1}{PrRe}\left(\frac{\partial^2 T^{+}}{\partial X^2}+\frac{\partial^2 T^{+}}{\partial Y^2}\right) \tag{3.4}$$

So, for the dimensionless variables, the expressions become:

$$U=\frac{u}{U_o},\quad V=\frac{v}{U_o},\quad X=\frac{x}{L},\quad Y=\frac{y}{L},\quad T^{+}=\frac{T-T_c}{T_h-T_c},\quad P=\frac{p}{\rho_{eff}U_o^2} \tag{3.5}$$

$$Re=\frac{U_o\,L}{\vartheta_f},\quad Pr=\frac{\vartheta_f}{\alpha_f},\quad Gr=\frac{g\beta L^3(T_h-T_c)}{\vartheta_f^2},\quad Ri=\frac{Gr}{Re^2} \tag{3.6}$$

Table 1. It presents the boundary conditions in dimensionless form. The symbol 'n' serves as a representation of the perpendicular orientation to the sloped walls.

Table 1. Boundary Conditions.

	V	U	Θ
Upper wall	0	1	0
Lower wall	0	0	0
Right & left walls	0	0	$\frac{\partial \theta}{\partial n} = 0$
Internal cylindrical wall	0	0	1

2.3. Thermal and Physical Characteristics of the Fluid Medium

Equations representing equivalent thermal characteristics were formulated and proven to be computationally efficient, as evidenced in [52-54]:

$$\rho_{hnf} = \left(1 - \varphi_{Cu} - \varphi_{Al_2O_3}\right)\rho_f + \varphi_{Cu}\rho_{Cu} + \varphi_{Al_2O_3}\rho_{Al_2O_3} \tag{3.7}$$

$$(\rho\beta)_{hnf} = \left(1 - \varphi_{Cu} - \varphi_{Al_2O_3}\right)(\rho\beta)_f + \varphi_{Cu}(\rho\beta)_{Cu} + \varphi_{Al_2O_3}(\rho\beta)_{Al_2O_3} \tag{3.8}$$

$$(\rho C_p)_{hnf} = \left(1 - \varphi_{Cu} - \varphi_{Al_2O_3}\right)(\rho C_p)_f + \varphi_{Cu}(\rho C_p)_{Cu} + \varphi_{Al_2O_3}(\rho C_p)_{Al_2O_3} \tag{3.9}$$

$$\frac{k_{hnf}}{k_f} = \frac{\frac{\varphi_{Al_2O_3}k_{Al_2O_3} + \varphi_{Cu}k_{Cu}}{\varphi} + 2k_f + 2\left(\varphi_{Al_2O_3}k_{Al_2O_3} + \varphi_{Cu}k_{Cu}\right) - 2\varphi k_f}{\frac{\varphi_{Al_2O_3}k_{Al_2O_3} + \varphi_{Cu}k_{Cu}}{\varphi} + 2k_f - \left(\varphi_{Al_2O_3}k_{Al_2O_3} + \varphi_{Cu}k_{Cu}\right) + \varphi k_f} \tag{3.10}$$

$$\mu_{hnf} = \mu_f \frac{1}{(1-\varphi)^{2.5}} \tag{3.11}$$

Table 2. Thermal and Physical Characteristics of H_2O, Cu, Al_2O_3 and H_2O- Cu -Al_2O_3 hybrid nanofluid [12].

Material	$k\ (W/m.K)$	$C_p\ (J/kg.K)$	$\rho\ (kg/m^3)$	$\beta\ (1/K)$	$\mu(Pa.s)$
H_2O	0.613	4179	997.1	21×10^{-5}	0.001003
Cu	441	385	8933	1.67×10^{-5}	-
Al_2O_3	40	765	3970	0.85×10^{-5}	-
H_2O – Cu - Al_2O_3 ($\Phi_{Cu} = 2\%$, $\Phi_{Al_2O_3} = 2\%$)	0.6889	3398.183	1215.276	1.68×10^{-4}	0.00111076
H_2O – Cu - Al_2O_3 ($\Phi_{Cu} = 3\%$, $\Phi_{Al_2O_3} = 3\%$)	0.7293	3104.249	1324.364	1.527×10^{-4}	0.0011707
H_2O – Cu - Al_2O_3 ($\Phi_{Cu} = 4\%$, $\Phi_{Al_2O_3} = 4\%$)	0.7714	2855.052	1433.452	1.394×10^{-4}	0.001235

2.4. Grid Generation

In two dimensional, grid computational generation allows for solving of the energy, momentum, and continuity equations of complex geometries. Volume meshing basically can be decomposed in to two types of approach that are structured grid and unstructured grid. These mathematical equations of structured grid are transformed into a surface-associated curvilinear coordinate system. However, for complicated geometries, mesh generation is necessary, which is time-consuming and often necessitates adjustments to the model's design. Thus, it is an advantageous selection for uncomplicated shapes. Still, it gets excessively inefficient and necessitates plenty of time for complicated shapes. Thus, it has been omitted from the current research. Unstructured grids are often more appropriate for complicated geometries, hence they are utilized in this study. The current work used a non-uniform, triangular, and unstructured discretization grid, as illustrated in Fig. 2.

2.5. Mesh Independence

An independency test for mesh has been carried out to determine the optimal number and size of mesh faces for this specific geometry. This study examines various element sizes: 1, 0.8, 0.6, 0.4, and 0.3, for radius ratio of 0.25 and Reynolds number of 100. The discretization mesh is non-uniform, triangular, and unstructured. Figure 3 illustrates the fluctuation of the mean Nusselt number with the element size. The element size of 0.3 yields nearly equal outcomes for the Nusselt number. Eventually, a mesh size of 43,660 elements had been used in this investigation as it represented the optimal balance between accuracy and computing efficiency.

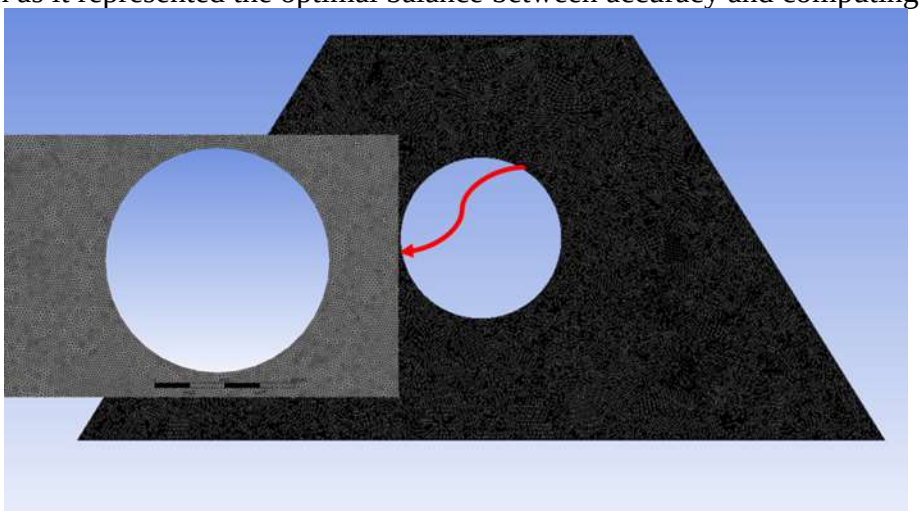

Figure 2. Mesh Generation.

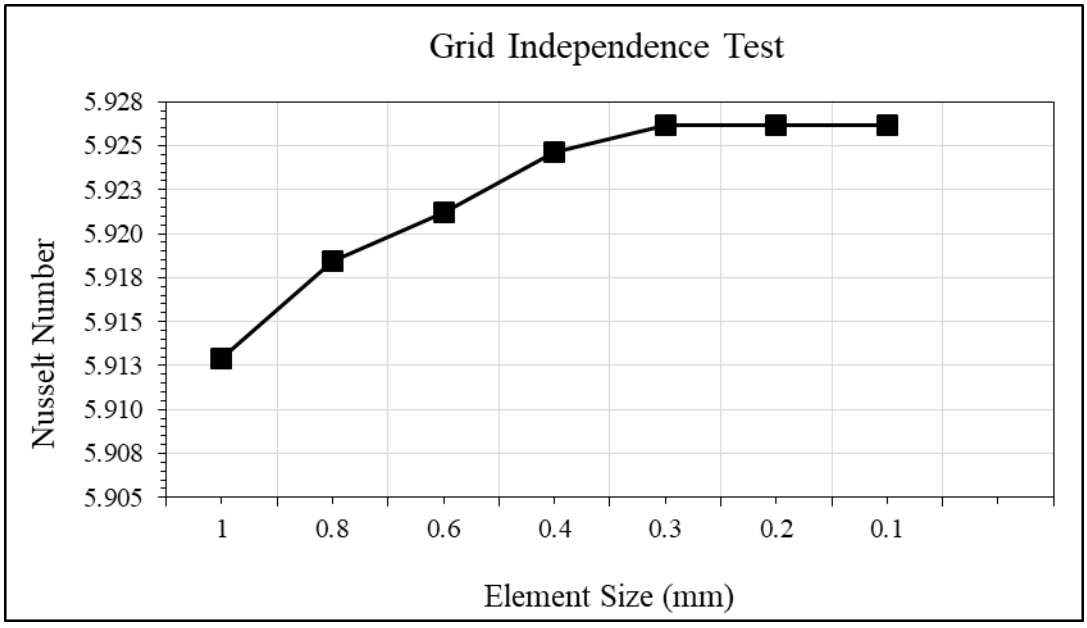

Figure 3. Element size and mean Nusselt number convergence.

2.6 Computational Approach

The solving methods may identify many factors related to the calculation's employed solving approach. The mathematical equations, under the specified boundary conditions, were resolved utilizing the ANSYS commercial software (ANSYS Fluent 2022 R1). At first, a mesh is constructed, then the ANSYS Fluent employs the solving algorithm to sequentially resolve the mathematical equations utilizing the SIMPLE algorithm. Furthermore, the rate of turbulent dissipation, momentum, pressure, and turbulent kinetic energy were all second order upwind in terms of spatial discretization. The SIMPLE formula is often used for solving the equations of Navier Stokes. The local Nu for the upper wall of the enclosure is presented by:

$$Nu_L = \frac{k_{eff}}{k_f}\frac{\partial\theta}{\partial Y}\Big|_{Y=1} \qquad (14)$$

The mean Nu for the heated cylindrical moving wall is presented by:

$$Nu_m = \int_0^1 Nu_L(X)\,dX \qquad (15)$$

3. Code Validation

The current simulation technique was validated using the streamline and isotherm outcomes reported in the research by Khanafer et al. [51]. Table 3 compares the mean Nusselt number values obtained from both studies. This investigation focused on analyzing the mixed convection airflow within a square enclosure in which the lower wall is hot, housing an internal cylinder that is circular with a RR=0.2. The employed medium was air with a Prandtl number of 0.7. Four Richardson number values were selected for this validation. The outcomes of validation revealed that the mean Nusselt number values from both simulations were highly similar, with an average relative difference of 1.62%.

Table 3. Validation of mean Nusselt number values for of the current project with the project of Khanafer et al. [51]

Richardson Number	$Nu_{previous}$[51]	$Nu_{current}$	Relative Diff. (%)
0.01	2.92	2.96	1.36%
1	3.50	3.60	2.85%
5	4.69	4.76	1.49%
10	5.04	5.08	0.79%

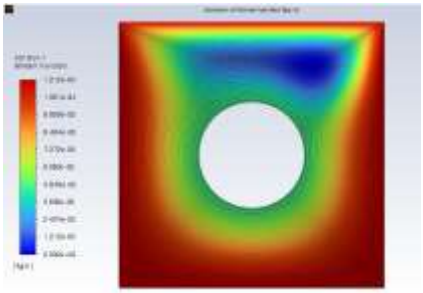
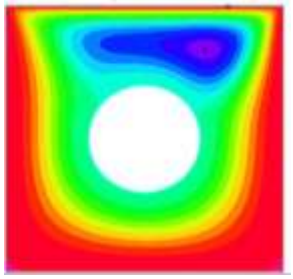

Ri = 0.01

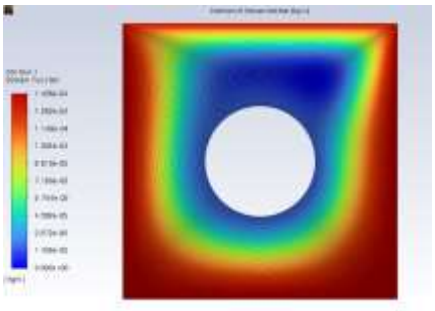


Ri = 1

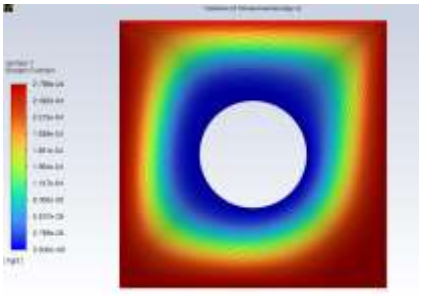
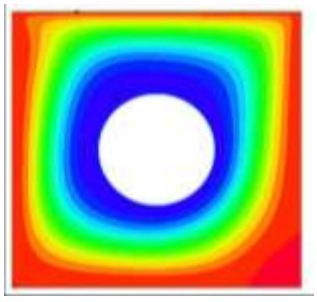

Ri = 5

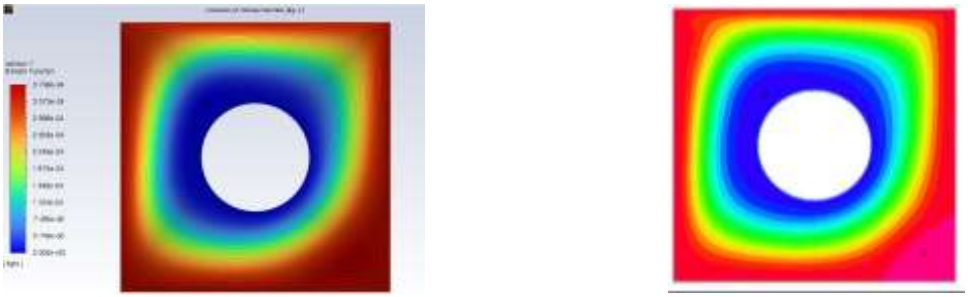

Ri = 10

Figure 4. Streamlines for the present simulation method (left) and Khanafer et al. work [51], (right).

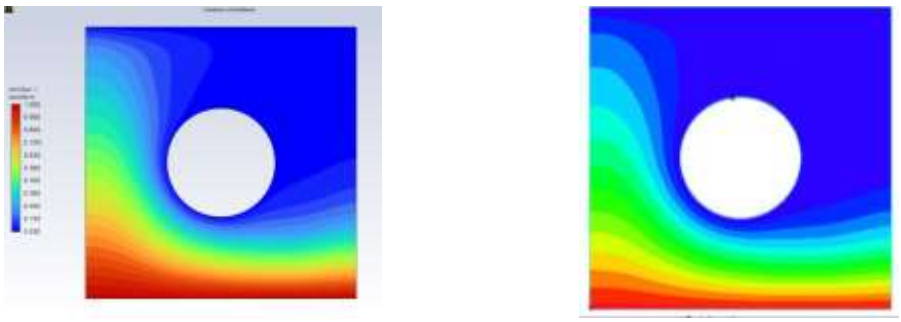

Ri = 0.01

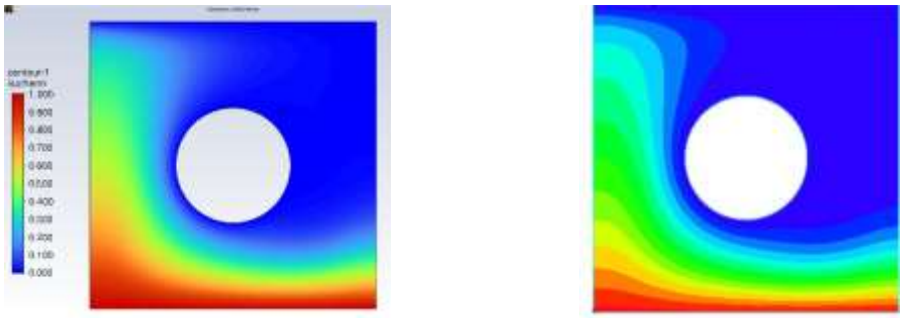

Ri = 1

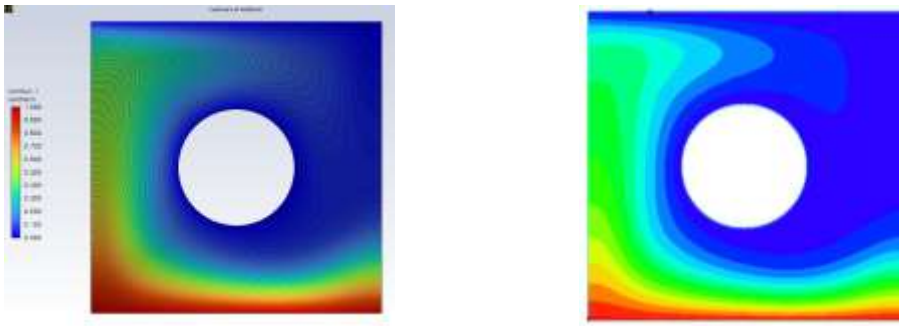

Ri = 5

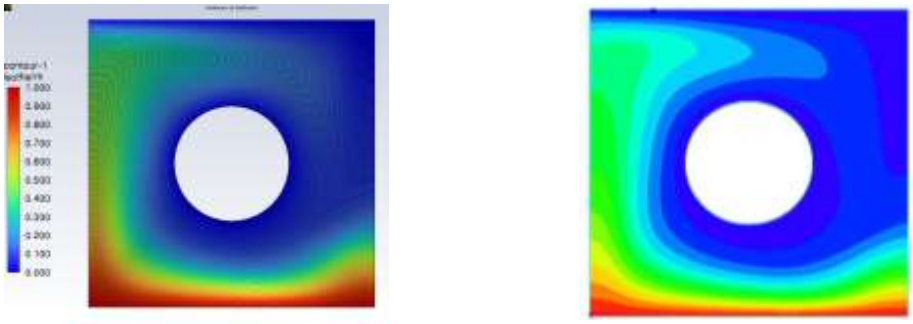

Ri = 10

Figure 5. Isotherms for the present simulation method (left) and Khanafer et al. work [51], (right).

4. RESULTS AND DISCUSSION

4.1 Streamline Maps and Isotherm Maps

Figure 6 illustrates Richardson number's influence over the flow lines and isothermal lines within a lid-driven hollow containing a hybrid nanoparticle volume percentage of 8% at various inclination angles (φ=0°, 45°, 90°, and 180°). In general, volume fractions, angles of inclination, as well as Richardson number have a significant influence on how flow lines and isothermal lines behave. The significance of natural convection in comparison to forced convection is indicated by the Richardson number, $Ri=Gr/Re^2$.

Figure 6 indicates that, for an inclination angle of 0° and Richardson number value of 0.01, a primary vortex is present with its center situated in the cavity's upper right side. The vortex rotation is clockwise, same direction as the motion. It spreads to the bottom right corner and appears to get stronger when Ri reaches 1 and 10, presumably due to the increased impacts of secondary flow caused by the intense free convection. In general, the fluid moves in the same direction by the moving wall. However, when the fluid comes into contact with the closest wall, its motion is changed to an opposed direction, creating a vortex, or a rotating motion.

When the Richardson number has a value of 0.01, the huge overall flow produced by the motion of the upper wall results in the primary flow pattern to fill the whole enclosure. Shear effects created by the movement of the upper wall are apparent at all inclination angles. Consequently, the isotherms showed a lack of development in the thermo-hydrodynamic boundary layers. Most of the isothermal lines were parallel with the thermal plum and weren't distorted. In the extensive recirculation zone, temperature gradients are minimal due to the efficient mixing of the liquid caused by the vigorous action of mechanically induced circulations. Consequently, the temperature variations within the enclosed region are minimal. As Richardson number rises, the temperature also rises, and the isothermal lines shift from the hot cylinder to the direction of the cold walls. As the Richardson number rises, the thermal plum becomes stronger. Its direction is primarily determined by the fluid type (both with and without the addition of hybrid nanoparticles), the Richardson number, and the inclination angle. Raising the Richardson number to 1 indicates that it is combined convection. In this case, there are two flows: the assisting flow and the opposing flow. When the main flow direction aligns with the buoyancy force direction (downward), the flow is termed assisting. When the direction of the inertia force (main flow) is upward, the flow is termed opposing. The type of flow is assisting in the current study.

Fig. 6 illustrates that when the inclination angle is 45°, the primary vortex spreads above the cylinder in alignment with the mobile wall at a Richardson number of 1. This indicates that the highest flow function is less strong when compared to the condition of the dominating forced convection at a Richardson number of 0.01. The intensity of the vortex amplifies with a rise in the main flow (by boosting the speed of the mobile wall and reducing Ri to 0.01), both with including and excluding the addition of hybrid nanoparticles within the base fluid. The vortex

splits into two powerful sections under conditions of a dominating free convection (Richardson number takes a value of 10) as a result of the strong free convection currents.

For an inclination angle of 90°, the pattern of streamlines closely resembles that for an inclination angle of 45°. The primary vortex divides into two weaker sections at a Richardson number of 1. However, the vortex remains powerful when the Richardson number is equal to 10, due to the dominant role of free convection. At a Richardson number of 0.01, the vortex appears more powerful than at a Richardson number of 1 but less so than at Richardson number of 10. Incorporating hybrid nanoparticles within the base fluid at a high volume percentage for a Richardson number of 10, generates prominent vortices and small vortices.

The streamlines within a lid-driven cavity including a bottom cylinder positioned with a radius ratio of 0.25 and an inclination angle of 180° are evident. The primary vortex is located beneath the heated cylinder and above the mobile wall at a Richardson number of 0.01, due to the increased shearing activity in this area resulting from a dominating forced convection. The vortex grows and expands with incorporating hybrid nanoparticles at a volume percentage of 8%, due to the significant influence of the main flow created by the movement of the lower wall. The primary vortex is split into vortices of varying intensities as Richardson number increases to 1. The highest stream function arises at the base of the cavity, over the mobile wall. The behavior in closed cavities differs from that of an open conduit when the main flow is reduced at the cost of the secondary flow. Two prominent vortices are observed on both sides of the lid-driven hollow. Compared to other Richardson number values, this is projected to produce a higher rate of heat transfer.

At a Richardson number of 10, the free convection takes over forced convection. Buoyancy enhances the main flow, hence strengthening convection flow as the Richardson number rises. Consequently, the isotherms intensify in proximity to the cold lid. Thermo-hydrodynamic boundary layer development will occur in parallel to the hot and cold walls. Furthermore, the highest temperature decreases, resulting in an increased heat transfer rate. Also, in the area close to the heated cylinder walls, it is clear that the isothermal lines created greater thermal gradients. The isothermal lines are spun around the heated cylinder, exhibiting curved lines capped by a thermal plume in a localized area adjacent to the hot wall. However, due to the dominant forced convection, these lines are distant from the hot cylinder surface and move closer to the cold walls. The generation of two plumes at a high Ri implies an increased rate of heat transfer inside a cavity that is lid-driven at an inclination angle of 180°. Increasing the percentage of volume for hybrid nanoparticles beyond 10%, is generally expected to cause a decrease in the liquid's thermal diffusivity as well as negative effects on flow stream and the transfer of heat within the cavity.

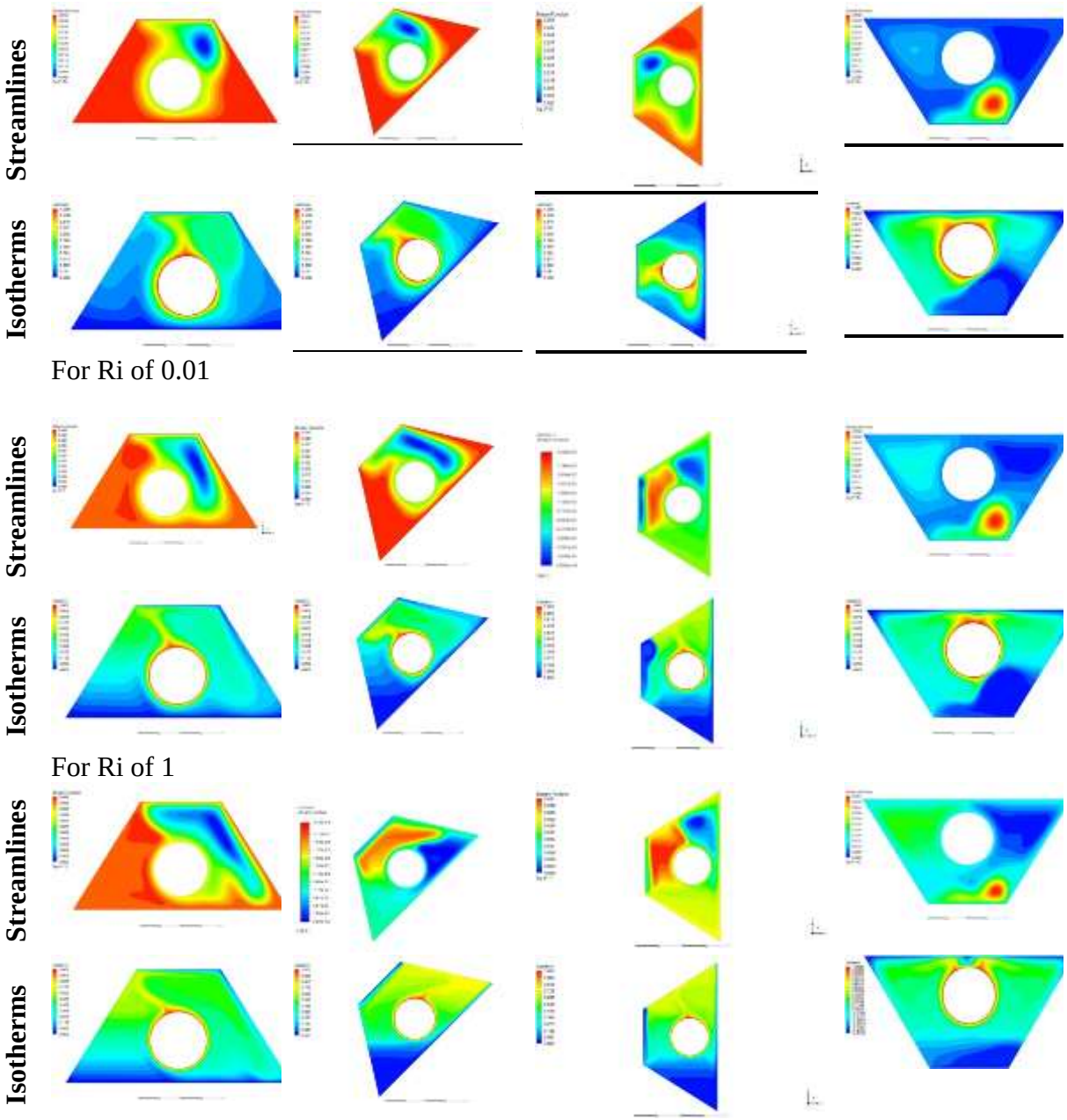

Figure 6. Streamline maps and isotherm maps within a lid-driven cavity including a cylinder positioned at the bottom with RR = 0.25 and ϕ = 0.08.

4.2 Mean Nusselt Number

Figure 7 illustrates the mean Nusselt number in relation to hybrid nanoparticles volume percentage for several Richardson number and cavity inclination angles (φ=0°, 45°, 90°, and 180°). It has been noted that when the Richardson number rises, the mean Nusselt number for every volume fraction ranges rises as well. The mean Nusselt number values for φ=180° exceed those for all other angles of inclination when Ri is equal to 10 & hybrid nanoparticles volume percentage are: 0%, 4%, and 6%. This pattern becomes reversed at ϕ=8%, where an inclination angle of 0°, yields the highest mean Nusselt number compared to other inclination angles. Consequently, the fluid's energy exchange rates will increase, which will improve the flow's thermal dispersion. For Ri=0.01 and φ=45°, the mean Nusselt number is reduced as the volume percentage increases from 6% to 8%. The high concentration of hybrid nanoparticles and the

moving wall's slanted direction work together to reduce the rate of heat transfer. Identical behavior is detected when the Richardson number is equal to 10 and φ=180°.

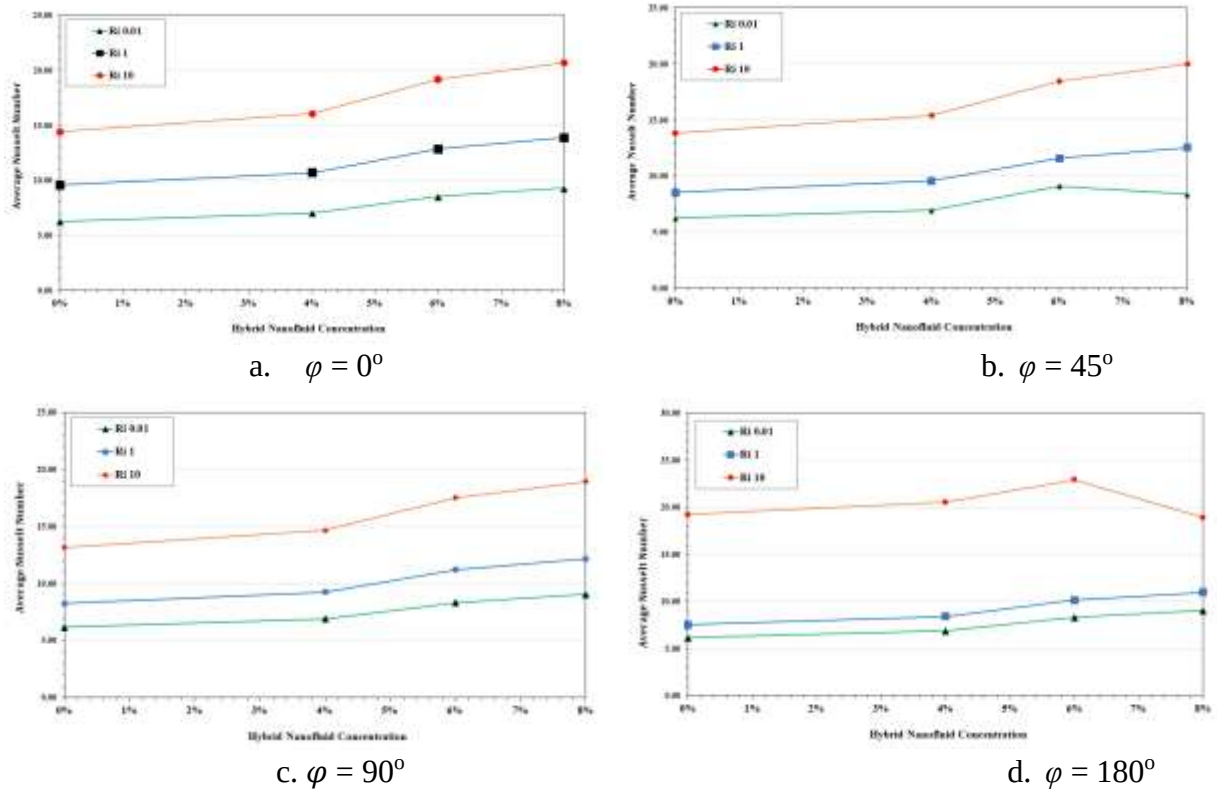

a. $\varphi = 0^o$ b. $\varphi = 45^o$

c. $\varphi = 90^o$ d. $\varphi = 180^o$

Figure 7. The mean Nusselt number surrounding the inner cylinder for different hybrid nanoparticle volume percentages and inclination angles.

4.3 Friction Losses

Figure 8 shows the pressure drop (indicating frictional losses) as a function of the volume percentage of hybrid nanoparticles, for various Richardson numbers (Ri) and cavity inclination angles (φ = 0°, 45°, 90°, 180°). The pressure drop increases slightly for Ri values of 0.01 and 1, but significantly rises for Ri value of 10 as the hybrid nanoparticle volume percentage rises. This is due to the increased viscosity from the added hybrid nanoparticles, which increases shear stress and frictional losses. However, at Ri value of 10 and an inclination angle of 180°, the pressure drop decreases with a rise in hybrid nanoparticle volume percentage from 6% to %8.
The pressure drop increases with the Richardson number (Ri) for angles of φ = 0°, 45°, and 90°, as shown in Figure 8. For Ri values of 0.01 and 1, pressure drop values are similar, suggesting they are effective in minimizing high pressure gradients. However, for Ri value of 10, the pressure drop is significantly higher, making it less desirable. In contrast, for an inclination angle of 180°, the behavior drastically changes. Mixed convection (Ri = 1) results in the lowest pressure drop, while forced convection (Richardson number has a value of 0.01) leads to the highest. Natural convection (Richardson number has a value of 10) falls in between these two cases.

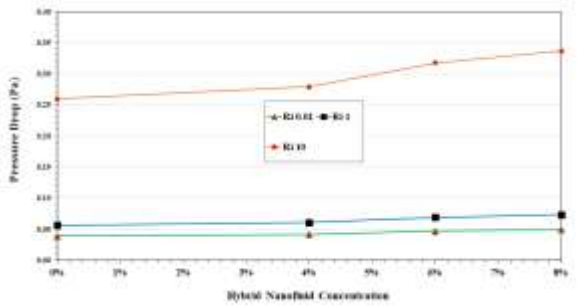

b. $\varphi = 0^o$

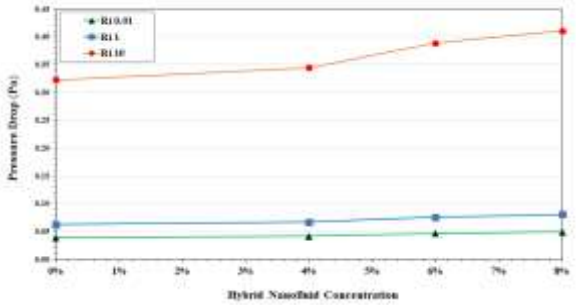

b. $\varphi = 45^o$

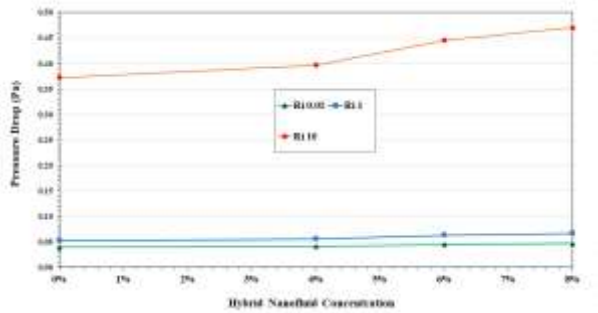

c. $\varphi = 90^o$

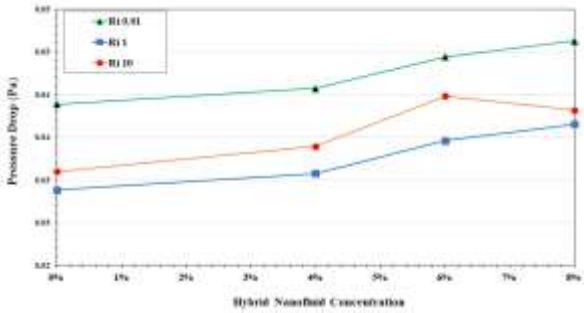

d. $\varphi = 180^o$

Figure 8. The pressure drop inside the cavity for different hybrid nanoparticle volume percentages and inclination angles.

5. Conclusions

1. The rate of heat transfer rises with the rise of Richardson number due to the increase of natural convection current.
2. The process of heat transfer is generally improved as the volume percentage of hybrid nanoparticle rises.
3. The growth in streamlines at Ri=1 and Ri=10 is far greater than when the Richardson number has a value of 0.01, particularly at an inclination angle of 0° and 180°.
4. The highest values of the maximum stream function arise for a Richardson number that has a value of 10 at all inclination angles and hybrid nanoparticle volume percentages.
5. Reducing the main flow at the cost of secondary flow in locked hollows produces behaviors contrary to that observed in open conduits.
6. The thermal plume is observed to rotate clockwise over the heated cylinder as Ri rises from 0.01 to 1.
7. Average Nusselt number for an inclination angle of 180° exceeds those for the other angles of inclination at a Richardson number of 10 and hybrid nanoparticle volume percentages of 0%, 4%, and 6%. This pattern is reversed at volume percentage of 8%, where an inclination angle of 0° yields the highest mean Nusselt number compared to other inclination angles.
8. It has been observed that the pressure drop rises as the Richardson number rises for an inclination angle of 0°, 45°, and 90° at Ri=10.
9. At an inclination angle of 180°, the mixed convection (Richardson number has a value of 1) is the best case that results in the lowest pressure drop. Conversely, forced convection (Richardson number has a value of 0.01) is the worst case that results in the largest pressure drop.

Abbreviations:

Al_2O_3 = Aluminum Oxide

H_2O = Water

Cu = Copper

CFD = Computational Fluid Dynamics

Gr = Grashof Number ($\frac{g\beta L^3(T_h - T_c)}{\vartheta_f^2}$)

h = Convective Heat Transfer Coefficient (W/m^2K)

C_p = Specific Heat ($J\ /\ kg.K$)

k = Thermal Conductivity ($W/m.K$)

g = Gravitational Acceleration (m/s^2)

Nu = Nusselt Number

Pr = Prandtl Number ($\frac{\vartheta_f}{\alpha_f}$)

Re = Reynolds Number ($\frac{U_o\ L}{\vartheta_f}$)

Ri = Richardson Number ($\frac{Gr}{Re^2}$)

RR = Radius Ratio

u = Velocity in x-axis (m/s)

U = Non-Dimensional Velocity in x-axis

U_o = Lid Velocity (m/s)

v = Velocity in y-axis (m/s)

V = Non-Dimensional Velocity in y-axis

T = Temperature (K)

T^+ = Dimensionless Temperature

P = Dimensionless Pressure

x, y = Space Coordinates

X, Y = Dimensional Space Coordinates

Greek Symbols:

α = Thermal Diffusivity ($k/\rho C_p$)

ρ = Density (kg/m^3)

β = Coefficient of Thermal Expansion (CTE) ($1/k$)

μ = Absolute Viscosity ($Pa.s$)

ν = Kinematical Viscosity (m^2/s)

ϕ = Volume Percentage of Nanoparticles

φ = Angle of Inclination (°)

Subscripts:

f = Base Fluid

hnf = Hybrid Nanofluid

T_c = Cold Temperature

T_h = Hot Temperature

References

[1] H. Nemati, M. Farhadi, K. Sedighi, E. Fattahi, A. A. R. Darzi. Lattice Boltzmann simulation of nanofluid in lid-driven cavity. International Communications in Heat and Mass Transfer 37 (2010) 1528–1534.

[2] M. M. Rahman, M. M. Billah, A. T. M. M. Rahman, M. A. Kalam, A. Ahsan. Numerical investigation of heat transfer enhancement of nanofluids in an inclined lid-driven triangular enclosure. International Communications in Heat and Mass Transfer, Volume 38, Issue 10, December 2011, Pages 1360- 1367.

[3] G.A. Sheikhzadeh, M. Ebrahim Qomi, N. Hajialigol, A. Fattahi. Numerical study of mixed convection flows in a lid-driven enclosure filled with nanofluid using variable properties. Results in Physics 2 (2012) 5–13.

[4] Hassan El Harfi, Mohamed Naïmi, Mohamed Lamsaadi, Abdelghani Raji, Mohammed Hasnaoui. Mixed Convection Heat Transfer for Nanofluids in a Lid-Driven Shallow Rectangular Cavity Uniformly Heated and Cooled from the Vertical Sides: The Opposing Case. Journal of Electronics Cooling and Thermal Control, 2013, 3, 111-130.

[5] H. Hassanzadeh Afrouzi and M. Farhadi. Mix Convection Heat Transfer in a Lid Driven Enclosure Filled by Nanofluid. Iranica Journal of Energy & Environment 4 (4): 376-384, 201.3

[6] Z. Said, H.A. Mohammed, R. Saidur. Mixed convection heat transfer of nanofluids in a lid-driven square cavity: A parametric study. International Journal of Mechanical and Materials Engineering (IJMME), Vol. 8 (2013), No.1, Pages: 48-57.

[7] Rehena Nasrin, M.A. Alim, Ali J. Chamkha. Modeling of mixed convective heat transfer utilizing nanofluid in a double lid-driven chamber with internal heat generation. International Journal of Numerical Methods for Heat & Fluid Flow Vol. 24 No. 1, 2014, pp. 36-57.
[8] Kourosh Javaherdeh, Mohammad Kalteh, and Touraj Azarbarzin. Mixed Convection Heat Transfer of a Nanofluid in a Lid-Driven Triangular Enclosure with Triangular Heat Source. Journal of Nanofluids,Vol. 3, pp. 1–9, 2014
[9] Mohammad Kalteh, Kourosh Javaherdeh, Toraj Azarbarzin. Numerical solution of nanofluid mixed convection heat transfer in a lid-driven square cavity with a triangular heat source. Powder Technology 253 (2014) 780–788.
[10] Anirban Chattopadhyay, Swapan K. Pandit, Sreejata Sensarma. Investigation on mixed convective heat transfer in a porous cavity with nanofluids. Conference: Sixth ICTACEM 2014. Indian Institute of Technology Kharagpur. December 2014.
[11] Abdelkader Boutra, Karim Raguia and Youb Khaled Benkahla. Numerical study of mixed convection heat transfer in a lid-driven cavity filled with a nanofluid. Mechanics & Industry 16, 505 (2015).
[12] Mahmudul Hasan Hasib, Md. Saddam Hossen, Sumon Saha. Effect of tilt angle on pure mixed convection flow in trapezoidal cavities filled with water- Al2O3 nanofluid. Procedia Engineering 105 (2015) 388 – 397.
[13] Abdelkader Boutra, Karim Ragui, Nabila Labsi, and Youb Khaled Benkahla. Lid-Driven and Inclined Square Cavity Filled with a Nanofluid: Optimum Heat Transfer. Open Eng. 2015; 5:248–255.
[14] Habib Salahi, Muhammad A. R. Sharif, Saeid Rasouli. Laminar Mixed Convective Heat Transfer in a Shallow Inclined Lid-Driven Cavity Filled with Nanofluid. Journal of Thermal Science and Engineering Applications DECEMBER 2015, Vol. 7.
[15] Zoubair Boulahia, Abderrahim Wakif, and Rachid Sehaqui. Mixed convection heat transfer of Cu-water nanofluid in a lid driven square cavity with several heated triangular cylinders. International Journal of Innovation and Applied Studies ISSN 2028-9324 Vol. 17 No. 1 Jul. 2016, pp. 82-93.
[16] Cimpean, D., M. Sheremet, and I. Pop, Mixed convection of hybrid nanofluid in a porous trapezoidal chamber. International Communications in Heat and Mass Transfer, 2020. 116: p. 104627.
[17] Ali, I., et al., Mixed convection in a double lid-driven cavity filled with hybrid nanofluid by using finite volume method. Symmetry, 2020. 12(12): p. 1977.
[18] Aljabair, S., A.A. Mohammed, and I. Alesbe, *Natural convection heat transfer in corrugated annuli with H2O-Al2O3 nanofluid.* Heliyon, 2020. **6**(11).
[19] Hakan F. Oztop. Combined convection heat transfer in a porous lid-driven enclosure due to heater with finite length. International Communications in Heat and Mass Transfer 33 (2006) 772–779.
[20] Hakan F. Oztop, Changzheng Sun, Bo Yu. Conjugate-mixed convection heat transfer in a lid-driven enclosure with thick bottom wall. International Communications in Heat and Mass Transfer 35 (2008) 779–785.

[21] C.Y. Wang. The recirculating flow due to a moving lid on a cavity containing a Darcy–Brinkman medium. Applied Mathematical Modeling 33 (2009) 2054–2061.
[22] Stephen Chung, Kambiz Vafai. Vibration induced mixed convection in an open-ended obstructed cavity. International Journal of Heat and Mass Transfer 53 (2010) 2703–2714.

[23] M.A. Mohd Irwan, A. M. Fudhail, C.S. Nor Azwadi and G. Masoud. Numerical Investigation of Incompressible Fluid Flow through Porous Media in a Lid-Driven Square Cavity. American Journal of Applied Sciences 7 (10): 1341-1344, 2010.
[24] M. A. Waheed, G. A. Odewole and S. O. Alagbe. Mixed convective heat transfer in rectangular enclosures filled with porous medium. ARPN Journal of Engineering and Applied Sciences, VOL. 6, NO. 8, AUGUST 2011.
[25] Wael M. El-Maghlany, Mohamed A. Teamah and Ahmed A. Hanafy Enhancement of Mixed Convection Heat Transfer in a Lid-Driven Square Cavity Completely Filled with Porous Material by Sidewalls Sinusoidal Heating. International Review of Applied Engineering Research. ISSN 2248- 9967 Volume 2, Number 1 (2012), pp. 55-84.
[26] Abdalla M. AlAmiri. Implications of placing a porous block in a mixed- convection heat-transfer, lid-driven cavity heated from below. Journal of Porous Media, 16 (4): 367–380 (2013).
[27] Anirban Chattopadhyay, Sreejata Sensarma and Swapan K Pandit. Numerical Simulations of Mixed Convection in a Porous Double Lid Driven Cavity. An International Conference on Mathematical Modeling And Computer Simulation with Applications, IIT Kanpur, December 31, 2013- January 2, 2014.
[28] Satyajit Mojumder, Sourav Saha, M. Rizwanur Rahman, M.M. Rahman, Khan Md. Rabbi, Talaat A. Ibrahim. Numerical study on mixed convection heat transfer in a porous L-shaped cavity. Engineering Science and Technology, an International Journal 20(1) August 2016. DOI: 10.1016/j.jestch.2016.07.005
[29] Majdı, H.S., et al., *Effect of fibrous porous material on natural convection heat transfer from a horizontal circular cylinder located in a square enclosure.* Journal of Thermal Engineering, 2021. **7**(6): p. 1468-1478.
[30] M. M. Billah, M. M. Rahman, Uddin M. Sharif, M.N. Islam," Numerical simulation on buoyancy-driven heat transfer enhancement of nanofluids in an inclined triangular enclosure. Procedia Engineering 90 (2014) 517–523.
[31] Raizah, Z., et al., MHD mixed convection of hybrid nanofluid in a wavy porous cavity employing local thermal non-equilibrium condition. Scientific Reports, 2021. 11(1): p. 17151.
[32] Salma Parvin and Rehena Nasrin. Magnetohydrodynamic Mixed Convection Heat Transfer in a Lid-driven Cavity with Sinusoidal Wavy Bottom Surface. Journal Tri. Math.Soci.12(2010) 1-9.
[33] Khaled Al-Salem, Hakan F. Oztop, Ioan Pop, and Yasin Varol. Effects of moving lid direction on MHD mixed convection in a linearly heated cavity. International Journal of Heat and Mass Transfer 55 (2012) pp. 1103–1112.
[34] Ziafat Mehmood and Tabish Javed. MHD-Mixed convection flow in a lid driven trapezoidal cavity under uniformly/ non-uniformly heated bottom wall. International Journal of Numerical Methods for Heat and Fluid Flow • May 2016 DOI: 10.1108/HFF-01-2016-0029.
[35] N. A. Bakar, A. Karimipour, and R. Roslan. Effect of Magnetic Field on Mixed Convection Heat Transfer in a Lid-Driven Square Cavity. Journal of Thermodynamics, Accepted 14 February 2016.
[36] M. Borhan Uddin, M. M. Rahman, M. A. H. Khan, R. Saidur, Talaat A. Ibrahim. Hydromagnetic double-diffusive mixed convection in trapezoidal enclosure due to uniform and nonuniform heating at the bottom side: Effect of Lewis number. Alexandria Engineering Journal (2016) 55, 1165–1176.
[37] M. Rashad, Sameh E. Ahmed, Waqar A. Khan, and M. A. Mansour. Inclined MHD Mixed Convection and Partial Slip of Nanofluid in a Porous Lid-Driven Cavity with Heat Source-Sink: Effect of Uniform and Non-Uniform Bottom Heating. Journal of Nanofluids, Vol. 6, pp. 1–11, 2017.

[38] Sameh E. Ahmed, Ahmed Kadhim Hussein, M.A. Mansour, Z.A. Raizah, & Xiaohui Zhang. MHD mixed convection in trapezoidal enclosure filled with micropolar nanofluids. Nanoscience and Technology: An International Journal 9(4):343–372 (2018).
[39] GH.R. Kefayati, H. Tang. MHD mixed convection of viscoplastic fluids in different aspect ratios of a lid-driven cavity using LBM. International Journal of Heat and Mass Transfer 124 (2018) 344–367.
[40] M. Humaun Kabir, M. Jahirul Haque Munshi, Nazma Parveen. Numerical Study of MHD Mixed Convection Heat Transfer of Nanofluid in a Lid-driven Porous Rectangular Cavity with Three Square Heating Blocks. AIP Conference Proceedings 2121, 070002 (2019); https://doi.org/10.1063/1.5115909.
[41] Md. Fayz-Al-Asada, M. A. Hossain, M. M. A. Sarker. Numerical Investigation of MHD Mixed Convection Heat Transfer Having Vertical Fin in a Lid-Driven Square Cavity. Cite as: AIP Conference Proceedings 2121, 030023 (2019); https://doi.org/10.1063/1.5115868, Published Online: 18 July 2019.
[42] Chin-Lung Chen , Chin-Hsiang Cheng. Experimental and numerical study of mixed convection and flow pattern in a lid-driven arc-shape cavity. Heat Mass Transfer (2004) 41: 58–66.
[43] M. A. R. Sharif. Laminar mixed convection in shallow inclined driven cavities with hot moving lid on top and cooled from bottom. Applied Thermal Engineering 27 (2007) pp. 1036–1042.
[44] Madhuchhand Bhattachary, Tanmay Basak, Hakan F. Oztop, Yasin Varol. Mixed convection and role of multiple solutions in lid-driven trapezoidal enclosures. International Journal of Heat and Mass Transfer 63 (2013) 366– 388.
[45] Chin-Lung Chen and Yun-Chi Chung. Numerical study on mixed convection heat transfer in inclined triangular cavities. Numerical Heat Transfer, Part A, 67: 651–672, 2015.
[46] Krunal M. Gangawane, Siddharth Gupta. Mixed convection characteristics in rectangular enclosure containing heated elliptical block: Effect of direction of moving wall. International Journal of Thermal Sciences 130 (2018) 100– 115.
[47] Litan Kumar Saha, Monotos Chandra Somadder, K. M. Salah Uddin. Mixed convection heat transfer in a lid driven cavity with wavy bottom surface. American Journal of Applied Mathematics 2013; 1(5): 92-101.
[48] A. R. M. Rosdzimin, S. M. Zuhairi and C. S. N. Azwadi. Imulation of mixed convective heat transfer using Lattice Boltzmann method. International Journal of Automotive and Mechanical Engineering (IJAME), ISSN: 1985- 9325(Print); ISSN: 2180-1606 (Online); Volume 2, pp. 130-143, July- December 2010.
[49] Mohammed, A., *Natural convection heat transfer inside horizontal circular enclosure with triangular cylinder at different angles of inclination.* Journal of Thermal Engineering, 2021. **7**(1): p. 240-254.
[50] A. FLUENT, 15.0 Theory Guide, Ansys Inc, 5 (2013).
[51] Khanafer, K., & Aithal, S. M. (2013). Laminar mixed convection flow and heat transfer characteristics in a lid driven cavity with a circular cylinder. International Journal of Heat and Mass Transfer, 66, 200-209.
[52] Brinkman, H.C. The viscosity of concentrated suspensions and solutions. J. Chem. Phys. 1952, 20, 571–581.
[53] Alsabery, A.I.; Hashim, I.; Hajjar, A.; Ghalambaz, M.; Nadeem, S.; Pour, M.S. Entropy Generation and Natural. Convection Flow of Hybrid Nanofluids in a Partially Divided Wavy Cavity Including Solid Blocks. Energies 2020, 13, 2942.
[54] El-Zahar, E., et al., Magneto-hybrid nanofluids flow via mixed convection past a radiative circular cylinder. Scientific Reports, 2020. 10(1): p. 10494.